2024 9th Asia Conference on Power and Electrical Engineering (ACPEE) | 979-8-3503-0963-8/24/$31.00 ©2024 IEEE | DOI: 10.1109/ACPEE60788.2024.10532462

Resilience Assessment of Regional Electric-Thermal Integrated Energy Systems Based on Diverse User Demands

Weiwei Wang
Zhongshan Power Supply Bureau of Guangdong Power Grid Co., Ltd
Zhongshan, China
2731799895@qq.com

Jianchu Liu
Zhongshan Power Supply Bureau of Guangdong Power Grid Co., Ltd
Zhongshan, China
935572859@qq.com

Zhaoxi Lin
Zhongshan Power Supply Bureau of Guangdong Power Grid Co., Ltd
Zhongshan, China
1073348589@qq.com

Xinghang Weng
Guangdong Power Grid Co. , Ltd.
Guangzhou, China
1372839573@qq.com

Jiawei Qu*
Key Laboratory of Smart Grid of Ministry of Education
Tianjin University
Tianjin, China
jiawei_qu@tju.edu.cn

Jie Du
Key Laboratory of Smart Grid of Ministry of Education
Tianjin University
Tianjin, China
jie_du@tju.edu.cn

***Abstract*—In recent years, the temporal and spatial infrastructure failures of regional integrated energy systems (RIES) due to various types of extreme natural disasters have been increasing, leading to significant impacts on social production and life. This paper proposes a resilience assessment system based on the demand of multiple users. Firstly, different heat loss coefficients are determined by the indoor temperature of various types of building users; secondly, the computation process of system resilience indexes is introduced by taking the ice hazard as an example; and lastly, the method proposed in this paper is tested in an integrated 9-node and 6-node electric-thermal network. The validity of the multivariate heat demand resilience assessment method is verified by the calculation case.**

Keywords—regional electric-thermal integrated energy system, user demands, resilience assessment

I. INTRODUCTION

Under the goals of "2030 carbon peak" and "2060 carbon neutral", China is accelerating the reform of the energy structure and building a clean and low-carbon energy system[1]-[3]. Regional integrated energy systems (RIES) have been developed greatly because of their advantages in meeting diversified energy needs and improving energy efficiency[4],[5], and it will become the mainstream form of the user side in the future. RIES has been developed greatly due to its strengths in satisfying diversified energy demand and improving energy utilization efficiency, so it will become the mainstream form of the user side in the future to meet the demand for cooling, heating and power supply as well as energy saving and emission shedding. However, in recent years, the frequency of extreme weather, due to ice, typhoons, high temperatures and other impacts caused by the number of park energy supply failure events is increasing, based on the above judgment, it is necessary to study the future energy system of multi-energy network load supply and demand coordination configuration, to further enhance the resilience of the system.

In this paper, the following studies are carried out with the electric combined heat and power integrated energy station as a unit: firstly, the thermal load regulation model considering user comfort is established based on the comfort difference of young, young, middle-aged and old groups; secondly, the multiple users are classified, and the demand response modeling is carried out for the residential, commercial and industrial users, so as to excavate the typical load curves of the different types of users, and lay the foundation of calculating the resilience indexes; then, the load supply and demand coordination configuration of the multi-energy network in the future energy system is necessary to further improve the system resilience level. Finally, taking the ice disaster weather as an example, the 9-node and 6-node electric-thermal integrated energy systems are combined to simulate the disaster situation. Through the analysis of the example, it is concluded that the heating comfort of each user group can be effectively improved after considering the demand of different user groups, and the value of the system resilience index can be reduced, which provides a data basis for the subsequent development of the corresponding economic upgrading strategy.

II. MODELING THE USER COMFORT FOR MULTIPLE AGE GROUPS

First, the thermal load regulation model considering user comfort is established based on the comfort differences among young, young, middle-aged and elderly groups. According to the literature [6], it is known that there is a significant correlation between age and thermal sensation, for example, the thermal unacceptability of elderly subjects is higher, and the differences between the elderly and young people in terms of thermal sensation and preference are more obvious. According to the World Health Organization's age

classification, users under 45 years of age are defined as young; users between 45 and 59 years of age are defined as middle-aged; users between 60 and 74 years of age are defined as younger older adults; users between 75 and 89 years of age are defined as elders; and users 90 years of age and older are defined as long-lived. The study showed that thermoneutral temperatures were the same up to age 45, generally defined as 20.4 °C; whereas, above age 45, so it can be seen that there is significant differences between the groups as age increases. The thermoneutral temperature for the 60-75 year old group was 21.2 °C, which is 0.7 °C higher than that of the 45-59 year old group (20.5 °C), and that for the 75-89 year old group (22 °C) it is higher than that of the 45-59 year old group (20.5 °C) by 1.5 °C. This implies that older people prefer to stay in warmer environments than younger people due to the different basal metabolic rates of different age groups in the same environment.

In addition, the existing buildings were categorized into industrial, commercial and residential loads, where the size of the industrial load is determined by its role, while the majority of the population in buildings such as commercial office buildings are young people, whose indoor temperature values are lower than those in residential buildings, which were set at 20.4 °C and 21.2 °C, respectively; and the residential loads were categorized into general residential loads and recreational medical resident load. Among them, the majority of the recreational and healthcare building population is over 70 years old, and the indoor temperature is defined as 22 °C.

Therefore, the limit temperature is set as 9 °C, 9.8 °C and 10.8°C in the commercial office buildings, residential buildings and the recreational and healthcare buildings.

III. Modeling of RIES

In order to centralize the clusters of buildings belonging to the users of all ages, this paper is proposed the RIES system which is schematized as Fig. 1[7].

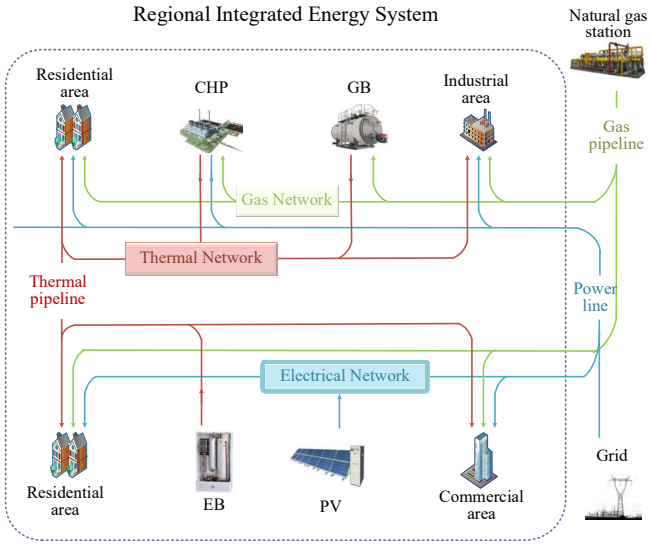

Fig. 1. Description of RIES.

In the picture, the coupling devices are the electrical boiler(EB) and the gas boiler(GB), the load required by the distribution network is provided by the superior grid, and the gas load is provided by the natural gas station. Furthermore, the residential area includes a general residential building and a recreational medical residential hospital.

IV. Modeling of Ice Storm Disasters

In the actual system, weather variations are not sharply demarcated between geographic regions. On long-distance transmission corridors, weather conditions are constantly changing over time and space, and are not exactly the same even within the same geographic region. This also makes the impact of weather on transmission lines/pipelines very complex and difficult to make accurate estimates. In order to evaluate the impact of weather on the transmission lines/pipelines more simply and effectively, the literature treats the adjacent area with approximate meteorological conditions as a weather region and assumes that the RIES in the same region are under the same weather conditions, and the same assumptions as in this paper are used[8].

The forces of ice cover and wind on the transmission line can be considered to be perpendicular to each other, as shown in Fig. 2.

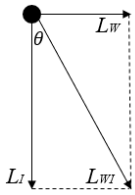

Fig. 2. Analysis of transmission line forces under ice damage.

In the above figure, L_I represents the ice force load (N/m), L_W stands for wind load (N/m).

As a result, the ice-wind force loads on the transmission line under the joint action of ice-wind force can be obtained based on the force synthesis.

$$L_{WI} = \sqrt{(L_I)^2 + (L_W)^2}$$

$$\begin{cases} L_I = 9.8\times10^{-3}\rho_I \pi (D + R_{eq})R_{eq} \\ L_W = CSv_g^{\ 2}(D + 2R_{eq}) \end{cases} \quad (1)$$

Where, C is the constant coefficient, D is the cable diameter (mm), S stands for the span factor, R_{eq} represents the thickness of ice cover (mm).

$$R_{eq} = \frac{T}{\pi\rho_I}\sqrt{(r\rho_W)^2 + (3.6vW)^2} \quad (2)$$

Where, T represents the duration of freezing rain in hours (h), r represents the rainfall rate (mm/h), ρ_I and ρ_W represents the density of ice, respectively, v represents the wind speed (m/s), which is taken as 1.5, and W represents the water content in the air, which is calculated by the formula $W = 0.067\times r^{0.864}$. Where, the gust wind speed v_g is calculated from Equation (3).

$$v_g = 1.29v + 12.9742 \quad (3)$$

The probability of failure p_f of a transmission line per unit length is:

$$p_f = \begin{cases} 0 & L_{\mathrm{WI}} \le a_{\mathrm{WI}} \\ \exp\left[\dfrac{0.6931(L_{\mathrm{WI}} - a_{\mathrm{WI}})}{b_{\mathrm{WI}} - a_{\mathrm{WI}}}\right] - 1 & a_{WI} < L_{WI} < b_{WI} \\ 1 & L_{WI} \ge b_{\mathrm{WI}} \end{cases} \quad (4)$$

Where, a_{WI} and b_{WI} are the first and second threshold values (N/m) for ice-wind loads, separately. The effects of wind and ice cover should be considered comprehensively when selecting the threshold values. In the separate consideration of wind speed, set the wind load of the two threshold values a_{W}, b_{W} were calculated by the wind speed of 1 times and 2 times the design value of wind speed; in the separate consideration of the ice cover, set the ice load of the two threshold values a_{I}, b_{I} were calculated by the thickness of the ice cover 1 times and 5 times the design value of ice cover thickness. Fault probability of transmission line per unit length. According to the probability of failure of a line of unit length, the probability of failure of a transmission line of length l can be calculated as:

$$p = 1 - (1 - p_f)^l \quad (5)$$

V. Indicator for Resilience Assessment

In order to measure the user-side heat load loss after failure, this section proposes the segmented heat loss coefficient c_{heat}, which takes the user-side indoor temperature as the starting point, and changes the basis of the failure state of the thermal system from heat load shedding to the user-side thermal comfort, and its segmentation is based on the PMV-PPD metrics mentioned in the previous section, and the principle is shown in Fig. 3. The specific definition is as followed[9].

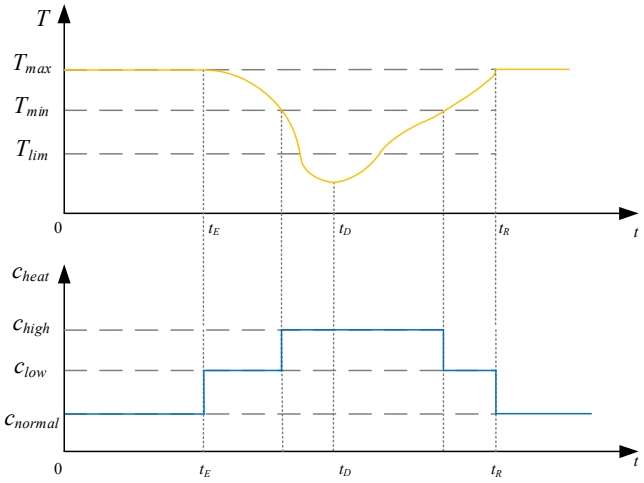

Fig. 3. Schematic diagram of segmented heat loss coefficients.

$$c_{heat} = f(T) = \begin{cases} c_{normal}, & T_{\min} \le T \le T_{\max} \\ c_{low}, & T_{\lim} \le T \le T_{\min} \\ c_{high}, & T \le T_{\lim} \end{cases} \quad (6)$$

In the formula, T_{min} and T_{max} interval between the user in the thermal comfort environment, corresponding to the weight of the heat loss can be ignored; T_{lim} and T_{min} interval users are more uncomfortable, the human body corresponds to the feeling of cool and warm, respectively, the stage of user heating has been affected to a certain extent c_{low}, so the corresponding heat loss should be taken into account as 1.5; when the indoor temperature is lower than the T_{lim}, the user side of the heating has been seriously affected, long time in the temperature may lead to the temperature-sensitive people (such as the old, young, pregnant, etc.) damage to the health, and therefore c_{high} should be added to the weight of the loss of the heat load under the temperature interval as 2.25.

The process of calculating the resilience indicator after adding the modified c_{heat} index can be expressed as follows. Establishing quantitative indicators is a necessary step in assessing and enhancing the resilience of the electric-thermal integrated systems against disasters. General resilience index consists of four key attributes: robustness, rapidity, redundancy, and sensitivity. The "4R" attributes is generally measured in terms of robustness and rapidity. In order to quantify these two assessment attributes, this paper adopts the resilience of the entire integrated energy systems based on the system's performance throughout the entire process of an extreme natural disaster, which improves the accuracy of the resilience assessment when the system is affected for a long period of time. Thus, the performance profile of the performance curve during extreme disasters can be described as $Q(t)$ in Fig. 4, Q_0 and $Q_{\min}$ represents the normal level and the most severe level of performance degradation, separately.

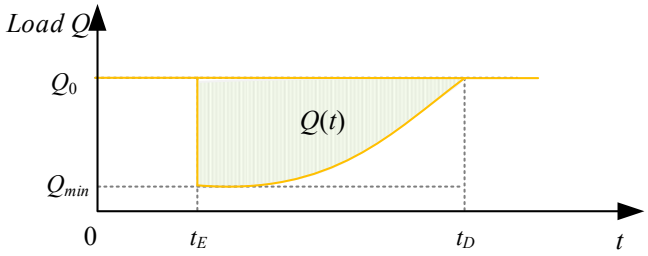

Fig. 4. Description of resilience assessment.

Therefore, the resilience index can be represented by R, considering that the thermal subsystem has thermal delay characteristics, the assessment object can consider of the indoor temperature deficit, so the indoor temperature change value and fault duration are used as the basis for assessing the system resilience.

$$R = \int_{t_1}^{t_2} c_{heat}^{t} \left[Q_0 - Q(t)\right] dt \quad (7)$$

$$r_{sys} = E[R] = \sum_{i \in I} p(i) R(i) \quad (8)$$

In the equation, R represents the amount of the electric-thermal coupled integrated energy systems load curtailment, measured in MW. I represents the number of lines in the RIES. A higher value of the resilience indicator implies that the system has suffered more damage, resulting in a larger load curtailment. This indicates a lower level of resilience in terms of the system's ability to withstand disasters.

VI. Case Analysis

An example of an integrated energy system coupled with a 9-node power system and a 6-node thermal system is

investigated, as shown in Fig. 5, where the coupling equipment is an electric boiler and a gas boiler, the RIES load is from [10]. In particular, H6 is the recreational and healthcare building, while H4 and H5 are the residential buildings.

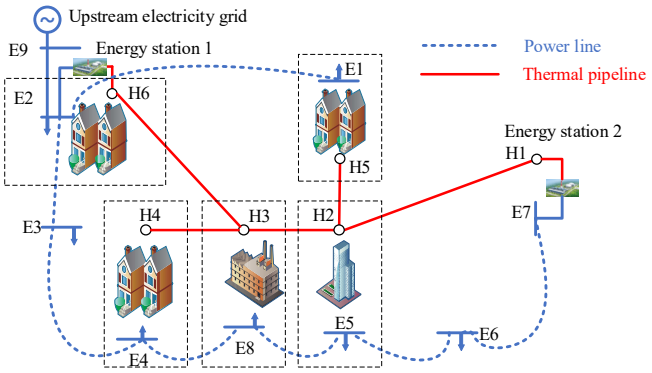

Fig. 5. Description of RIES.

We assume that the repair time of the upper distribution network and the natural gas station is a randomly generated integer between 24 and 48 h, and the failure time of the remaining branches is a random number between 1 and 5 h. The results are shown in Tab. I, ignoring the second-order effects. a_{WI} is set as 4(mm) and b_{WI} is set as 16(mm). When emergency response and recovery begins, the thickness of ice on the network is displayed to the operator and the probability of failure can be calculated for each distribution line.

TABLE I. FAILURE LINE NUMBER AND REPAIR TIME

Number	E9-E2, E2-E1, E2-E3, E3-E4, E4-E8, E8-E5, E5-E6, E6-E7, H1-H2, H2-H3, H3-H4, H3-H6, H2-H5
Repair time	1,2,2,2,2,2,2,2, 1,3,3,4,5

For example, RIES is affected by the ice storm from the 36 h. According to [9], it can be calculated that the curve of indoor temperature change in the building after the disaster of each thermal subsystem node, and the indoor temperature of each building is shown in Fig.6.

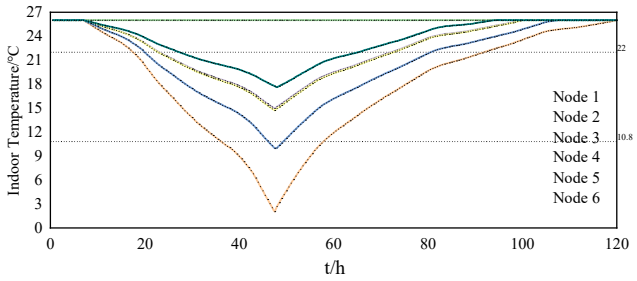

Fig. 6. The indoor temperature.

The following two assessment options are assumed, option 1 for resilience assessment without considering user demand; and option 2 for resilience index calculation considering different user demands. Since the indoor temperature of each building is mainly caused by the different loads of heat network, the load shedding of each heat network node is mainly introduced in the following.

First of all, option 1 is evaluated without considering the user demand at each node, in which the load shedding at each heat network node is shown in the Fig.7.

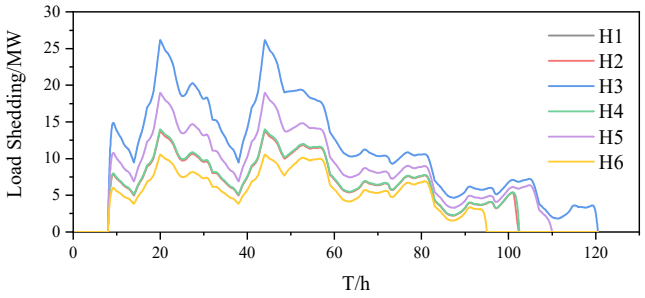

Fig. 7. The load shedding of option 1.

Secondly, option 2 is evaluated by considering the demand of users at each node and the load shedding at each heat network node are shown in Fig.8. Comparison of Fig. 8 with Fig. 7 shows that the variation in load shedding corresponding to the different heat network nodes varies considerably.

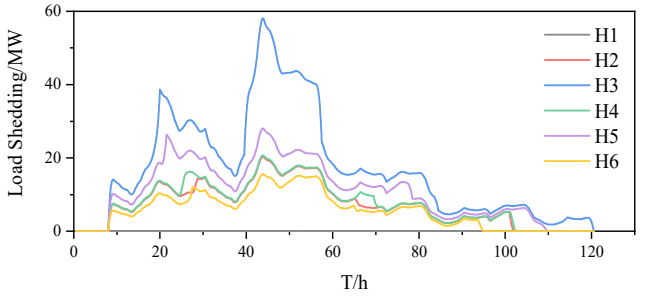

Fig. 8. The load shedding of option 2.

Calculation of resilience indicators for systems subjected to the ice hazard and the results are summarized in the Tab. II and Tab. III.

TABLE II. THE RESILIENCE INDEXES OF OPTION 1

Faulty Branch	E9-E2	E2-E1	E2-E3	E3-E4	
Resilience Indexes	165.76	165.63	158.96	152.72	
Faulty Branch	E4-E8	E8-E5	E5-E6	E6-E7	
Resilience Indexes	135.00	126.92	108.55	65.70	
Faulty Branch	H1-H2	H2-H3	H3-H4	H3-H6	H2-H5
Resilience Indexes	132.78	104.3	29.04	21.81	39.16

TABLE III. THE RESILIENCE INDEXES OF OPTION 2

Faulty Branch	E9-E2	E2-E1	E2-E3	E3-E4	
Resilience Indexes	173.18	173.05	166.38	160.14	
Faulty Branch	E4-E8	E8-E5	E5-E6	E6-E7	
Resilience Indexes	142.42	134.34	115.97	73.12	

Faulty Branch	H1-H2	H2-H3	H3-H4	H3-H6	H2-H5
Resilience Indexes	183.15	147.9	37.09	27.32	52.34

TABLE IV. THE RESILIENCE INDEXES COMPARISONS

Faulty Branch	H1-H2	H2-H3	H3-H4	H3-H6	H2-H5
Rate of change/%	37.93	41.80	27.72	25.26	33.66

Tab. 4 compares the quantities of thermal subsystem resilience indexes in option 1(from Tab. II) and option 2(from Tab. III). From the Tab. IV, it can be seen that after considering the user demand, the electric load shedding of the system is almost unchanged, but the thermal load shedding increases substantially, because the load shedding caused in the thermal branch is prone to cause a significant drop in the indoor temperature, and at this time, the range of changes in the user's tolerance is wider, and the amount of the load shedding affected by the indoor heat demand of the diversified users is consequently increased.

Through the comparison of options 1 and 2, it can be seen that in the resilience assessment proposed in this paper, which considers the demand of multiple users, the amount of emergency repair loads in the weak links of the grid after the onset of extreme natural disasters is elevated, and the weak links of the electric-thermal integrated energy system are emphasized, which lays down a modeling foundation for the repair sequence in the subsequent resilience restoration phase.

Meanwhile, since there are other coupled devices in the electric-thermal integrated energy system, the heat demand of the coupled system affected by other extreme disasters will continue to be expended in our future paper.

VII. CONCLUSIONS

This paper proposes a resilience assessment system for the regional integrated energy system under the influence of ice disaster. Firstly, the resilience assessment indexes considering users demand are established to assess the thermal demand of users in different buildings with different ages. Then, the resilience index is determined based on the ice disaster failure probability model, and it is demonstrated by the simulation results that the method proposed in this paper can be effectively identify diversified user demands and focus on the weaknesses of the thermal use of the system to enhance the system's resistance to ice storms.

ACKNOWLEDGMENT

This paper is supported by Science and Technology Project of China Southern Power Grid Corporation (032000KK52222022).

REFERENCES

[1] X. Fu and Y. Zhou, "Collaborative Optimization of PV Greenhouses and Clean Energy Systems in Rural Areas," in IEEE Transactions on Sustainable Energy, vol. 14, no. 1, pp. 642-656, Jan. 2023.

[2] M. Purlu and B. E. Turkay, "Optimal Allocation of Renewable Distributed Generations Using Heuristic Methods to Minimize Annual Energy Losses and Voltage Deviation Index," in IEEE Access, vol. 10, pp. 21455-21474, 2022.

[3] W. Xiaojin, S. Shucai, X. Yehua, J. Tao and L. Hongkun, "Research on Data Standardization and Unified Data Interface Based on Digital Station System," 2022 IEEE 5th Advanced Information Management, Communicates, Electronic and Automation Control Conference (IMCEC), Chongqing, China, 2022, pp. 1372-1376.

[4] Y. Wang, J. Hu and N. Liu, "Energy Management in Integrated Energy System Using Energy–Carbon Integrated Pricing Method," in IEEE Transactions on Sustainable Energy, vol. 14, no. 4, pp. 1992-2005, Oct. 2023.

[5] N. Liu, L. Tan, H. Sun, Z. Zhou and B. Guo, "Bilevel Heat–Electricity Energy Sharing for Integrated Energy Systems With Energy Hubs and Prosumers t," in IEEE Transactions on Industrial Informatics, vol. 18, no. 6, pp. 3754-3765, June 2022.

[6] B. Dong, C. Shang, M. Tong and J. Cai, "Analysis of the Influence of Age on Human Thermal Comfor," in International Conference on Construction and Real Estate Management 2020(ICCREM), Oct. 2022, pp. 170-176.

[7] L. Guo, L. Wang, W. Wei and J. Wu, "Day Ahead Economic Dispatch of District Integrated Energy Service Providers under Energy Market," in 2019 IEEE 3rd International Electrical and Energy Conference (CIEEC), Beijing, China, 2019, pp. 1878-1883.

[8] N. Zhao, K. Hou, X. Yu and H. Jia, "Full-Time Scale Resilience Enhancement Framework for Power Transmission System Under Ice Disasters," in International Journal of Electrical Power & Energy, vol. 126, March 2021.

[9] K. Hou, Y. Zhu and X. Xu, "Impact of Heat Supply Delays and Human Safety on the Reliability of Urban Energy Systems," in 2022 IEEE Power & Energy Society General Meeting (PESGM), Denver, CO, USA, 2022, pp. 1-5.

[10] P. Saini and L. Gidwani, "An investigation for battery energy storage system installation with renewable energy resources in distribution system by considering residential, commercial and industrial load models," in Journal of Energy Storage, vol. 45, Jan. 2022.